



Bimetallic Ni–Cu/CeO₂–Al₂O₃ catalysts for conversion of ethanol to higher alcohols

Vinayagamoorthi Rathinasamy^{1,2} · Ariharan Arjunan² ·
Krishnamurthy Konda Ramaswamy² · Viswanathan Balasubramanian² ·
Shanthi Kannan¹

Received: 15 September 2022 / Accepted: 4 January 2023
© Akadémiai Kiadó, Budapest, Hungary 2023

Abstract

A sustainable route for the synthesis of butanol and higher alcohols via condensation of bio-ethanol has been investigated on a series of modified nickel on alumina catalysts. To maximize the selectivity for butanol, alumina support has been modified with ceria (5 wt% of alumina) to enhance basicity. Copper is added as the second metal, to promote dehydrogenation-hydrogenation functionality. Ni–Cu bi-metallic catalysts with varying proportions of the metals, i.e., bimetallic 5.5% Cu–2.5% Ni, 4% Cu–4% Ni and 2% Cu–6% Ni catalysts and 8% Cu, 8% Ni (all wt%) mono metallic catalysts, supported on ceria modified Al₂O₃, have been prepared by wet impregnation and characterized by XRD, BET, TEM, NH₃- and CO₂ TPD, H₂-TPR and XPS. Condensation of ethanol has been carried out in Parr reactor, in batch mode (8 h, at 200 °C, after pressurization with nitrogen (10 bar). Mono metallic Ni displays ethanol conversion of 41%, with butanol selectivity of 48.6%. Whereas, mono metallic Cu catalyst, under identical reaction conditions, displays high butanol selectivity (64%) but very low ethanol conversion (18%). Bimetallic catalyst with composition 5.5% Cu–2.5% Ni, displays higher butanol selectivity of 55.6% with conversion at 32.2%. Thus, by optimization of Cu and Ni composition and support

✉ Shanthi Kannan
kshanthiramesh@yahoo.com; shanthiramesh@annauniv.edu

Vinayagamoorthi Rathinasamy
vgmsathish@gmail.com

Ariharan Arjunan
ariharanmsc87@gmail.com

Krishnamurthy Konda Ramaswamy
krkonda1949@gmail.com

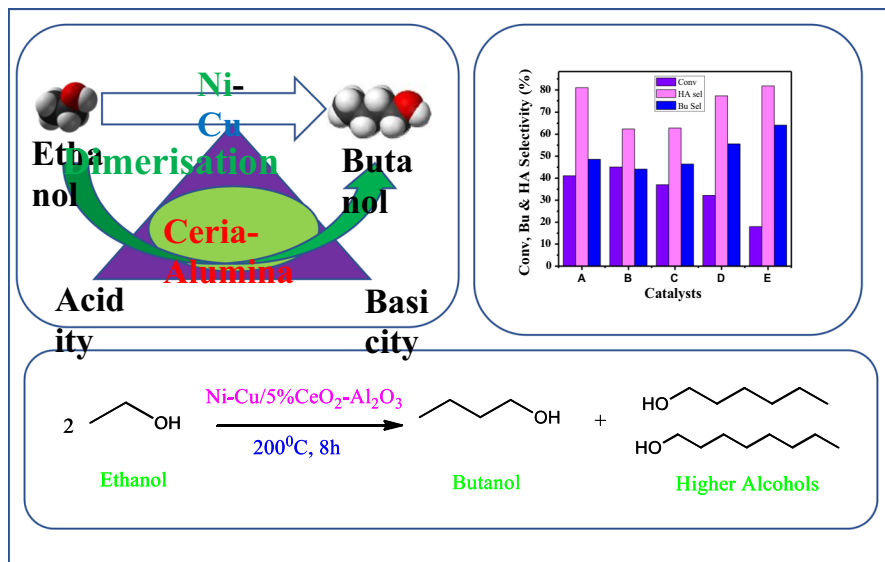
Viswanathan Balasubramanian
bviswanathan@gmail.com

¹ Department of Chemistry, Anna University, Chennai 600025, India

² National Center for Catalysis Research, Indian Institute of Technology, Madras, Chennai 600036, India

acidity/basicity, it is possible to maximize butanol selectivity. XPS and TPR studies indicate Ni–Cu alloy formation, especially in the compositions, 4% Ni–4% Cu, and 2.5% Ni–5.5% Cu. Presence Ni–Cu alloys, moderation of acidity and increase in medium and strong basic sites facilitate higher butanol selectivity.

Graphical Abstract



Keywords Guerbet reaction · Ethanol to butanol · Cu-Ni bimetallic catalyst · Cu-Ni alloy · Ceria-alumina support

Introduction

Availability of bio-ethanol in large quantities from various biomass resources has led to the revival of Guerbet alcohol chemistry [1]. Ethanol undergoes catalytic condensation to yield butanol and C_4+ carbon number alcohols. Butanol, considered as the future biofuel [2, 3] is bestowed with several advantages over ethanol, such as, higher energy density, lower volatility and solubility in water, non-corrosive nature, facile blending with gasoline and rendering more efficient combustion (Table S1) [4–7]. C_4+ alcohols find wide-spread applications as feedstocks, chemical intermediates and in polymers, surfactants and detergent industries [8]. Conversion of ethanol to butanol and higher alcohols through Guerbet chemistry has opened up another route for ethanol to jet fuel (ETJ) production [9]. C_4 – C_6 alcohols undergo sequential dehydration to the corresponding olefins, followed by oligomerization of olefins and hydrogenation of long chain olefins, to yield bio-jet fuel/Sustainable Alternative Jet Fuel (SAF). Globally, all

major airlines are planning to gradually replace fossil derived ATF (Aviation Turbine fuel) with SAF, so as to meet the mandated reduction in emission levels by 2050 [10].

Detailed reviews [11–13] on different heterogeneous and homogeneous catalysts, process features and recent developments on ethanol conversion to butanol and higher alcohols have been published. Transition metals (Ni, Cu, Co, Ru, Rh Au etc.,) on different types of supports have been explored extensively for this process. Especially, alumina supported nickel catalysts, which possess metal (for dehydrogenation hydrogenation functions) and acidic-basic sites (for aldol condensation function) display high activity and selectivity for C_4 +alcohols formation Table S.2. Similarly, copper-based catalysts on various supports also display high activity and selectivity for conversion of ethanol. A list of copper-based mono and bi-metallic catalysts investigated for conversion of ethanol has been compiled and presented in Table S.3. Though a variety of supports have been explored for mono metallic copper catalysts, Ceria modified carbon is found to be highly effective with a maximum ethanol conversion of 45–46% and butanol selectivity of 41–42%. However, reaction temperature is high at 250 °C. Among the bi-metallic catalysts, In-Cu and Pd-Cu display moderate selectivity, but lower ethanol conversion. Bi-metallic Cu-Ni (with higher metal loading (20%) and narrow variation in composition on Mg-Al-O support) and supported on porous metal oxides (PMO) exhibit high conversion (47.9%) and butanol selectivity (72%) but at very high reaction temperature (310 °C) and pressure (80 bar) in condensed phase [14]. Trimetallic Cu-Ni-Mn shows moderate activity (30%) and butanol selectivity of 39%.

Earlier work [15] on Ni-Co bimetallic catalysts supported on ceria modified alumina, has shown that the bimetallic catalysts with specific compositions of Ni and Co display higher activity and selectivity compared to the respective mono metallic catalysts. Superiority of bi-metallic Ni-Co catalysts is attributed to the formation of Ni-Co alloys and increase in reducibility of Ni. On similar grounds, studies on bi-metallic Ni-Cu catalysts with varying proportions (wt%) of the metals, bi-metallic 6%Ni-2%Cu, 5.5%Ni-2.5% 4%Ni-4% Cu and Ni (8%) and Cu (8%) mono metallic catalysts, supported on ceria (5 wt%)-alumina have been carried out in order to develop catalysts with better performance. This aspect of Ni-Cu catalysts, with varying proportions of Ni and Cu, for condensation of ethanol at lower reaction temperature have not been explored so far. Secondly, the use of Cu in combination will be beneficial as compared with Ni-Co system. Sun et al. [14] have investigated only Ni-Cu catalysts with high metal loading and narrow variation in compositions. All the catalysts have been prepared by wet impregnation and characterized by X-ray diffraction, Temperature Programmed Reduction (TPR), X-ray Photoelectron Spectroscopy (XPS), acidity and basicity measurements. Ethanol conversion reactions were carried out in 100 ml Parr reactor, in batch mode, at 200 °C for 8 h, after pressurization with nitrogen up to 10 bar [16].

Experimental

Chemicals

Boehmite (AlOOH) (Pural SB, Sasol, Germany), Nickel nitrate hexahydrate $\text{Ni}(\text{NO}_3)_2 \cdot 6\text{H}_2\text{O}$, Copper nitrate hexahydrate $\text{Cu}(\text{NO}_3)_2 \cdot 6\text{H}_2\text{O}$, Cerium nitrate hexahydrate ($\text{Ce}(\text{NO}_3)_2 \cdot 6\text{H}_2\text{O}$) (99.9%, CDH), were used as such. Absolute alcohol (99.9%) from Changshu Hongsheng Fine Chemical Co. Ltd., China, was used as such for carrying out reactions.

Preparation of support and catalysts

Gamma alumina ($\gamma\text{-Al}_2\text{O}_3$) was prepared by calcination of boehmite (AlOOH) at 450 °C for 4 h. Al_2O_3 was impregnated separately with required quantity of cerium nitrate $\text{Ce}(\text{NO}_3)_2 \cdot 6\text{H}_2\text{O}$, (to obtain 5 wt% of ceria in alumina) dissolved homogeneously in 20 mL of distilled water. After evaporation of excess water, the slurry was dried in air at 120 °C for 12 h and then calcined at 600 °C for 12 h in N_2 atmosphere. Ni (2.5% to 8 wt%) and Cu (2 to 8 wt%) as nickel nitrate and copper nitrate, respectively, were loaded on ceria modified alumina by wet impregnation, dried at 120 °C for 12 h, followed by reduction in H_2 flow at 500 °C for 12 h (19).

Characterization of catalysts

Powder XRD diffraction patterns for the catalysts were recorded using Rigaku Corporation, Japan, Model Miniflex IIX-ray diffractometer, with $\text{Cu K}\alpha$ ($\lambda = 0.15418$ nm) radiation in the 2θ range of 10° to 80° and at a scan rate of 3°/min. Ni crystallite size of the catalysts were calculated by X-ray line broadening analysis, using Debye-Scherrer equation.

N_2 adsorption and desorption isotherms were measured at -196 °C using a Micromeritics ASAP 2020 unit. Surface area of the catalysts were measured by BET method and pore volume and pore size distribution by BJH method.

Temperature programmed reduction (TPR) and temperature programmed desorption (TPD) of ammonia and carbon dioxide were performed on Chem. BET TPR/TPD Chemisorption Analyzer (Quanta Chrome Instruments, USA) equipped with a thermal conductivity detector (TCD). For TPR measurements, the catalysts were calcined in air at 300 °C, prior to TPR experiments. 50 mg of calcined catalyst was pre-treated at 300 °C in high purity Ar gas (25 cm^3/min) for 1 h and then cooled to room temperature in Ar flow. The gas was changed to 10% H_2 in Ar (25 cm^3/min) at room temperature. After the stabilization of the baseline, TPR patterns were recorded from room temperature to 800 °C with a heating rate 10 °C/min.

For TPD of ammonia, 50 mg of the reduced catalyst was pretreated at 300 °C in helium flow of 20 mL/min for 1 h and cooled to room temperature in helium flow. The sample was saturated with ammonia by passing 10% NH_3 in helium gas over the catalyst for 20 min. After flushing out weakly adsorbed ammonia with helium

flow at 100 °C, the base line was established. TPD of adsorbed ammonia was then recorded by heating the sample in helium flow up to 650 °C with a heating rate of 10 °C/min. For TPD of CO₂ similar procedure was adopted using CO₂ as probe molecule instead of ammonia.

X-ray photoelectron spectra of the reduced catalysts were recorded using Omicron Nanotechnology, Oxford Instruments, UK, instrument with Mg K_α radiation. The base pressure of the analysis chamber during the scan was 2×10^{-10} mbar. The pass energies for individual scan and survey scan are 20 and 100 eV. The spectra were recorded with step width of 0.05 eV. The data were processed with the Casa XPS software.

Evaluation of catalysts for ethanol conversion

Details on the evaluation of catalysts and the methods followed in GC analysis of reaction products and activity/selectivity calculations are carried in the usual manner and details can be available in in an earlier publication [16].

Results and discussion

Characterization of catalysts

X-ray diffraction (XRD)

XRD patterns for the three Ni–Cu bimetallic catalysts along with those for 8%Cu/5%CeO₂–Al₂O₃ and 8%Ni/5%CeO₂–Al₂O₃ mono metallic catalysts are presented

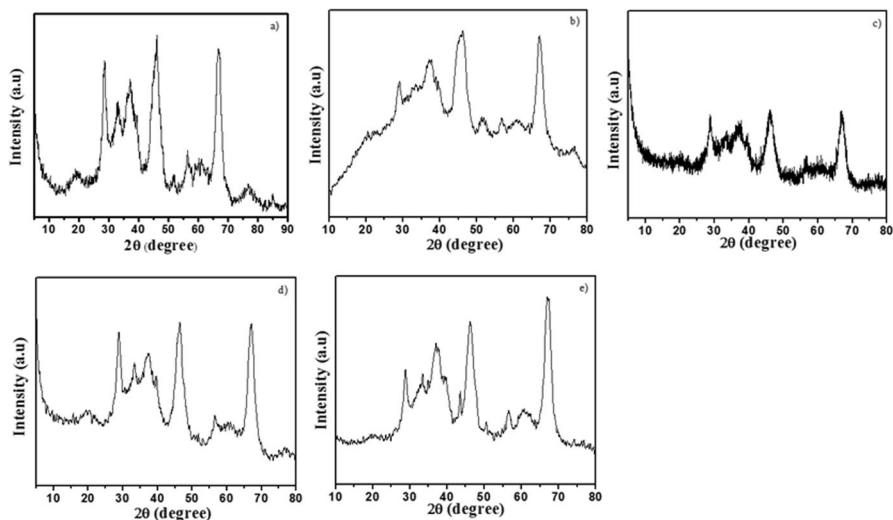


Fig. 1 XRD patterns for Ni-Cu bimetallic catalysts, **a** 8%Ni/5%CeO₂-Al₂O₃, **b** 6%Ni-2%Cu/5%CeO₂-Al₂O₃, **c** 4%Ni-4%Cu/5%CeO₂-Al₂O₃, **d** 2.5%Ni-5.5%Cu/5%CeO₂-Al₂O₃, **e** 8%Cu/5%CeO₂-Al₂O₃

in Fig. 1. Diffractogram for 8% Ni/5% CeO₂-Al₂O₃ displays all the characteristic d-lines of gamma alumina, ceria and Ni metal. All major d-lines, observed at 2θ = 18.8°, 36.8°, 45.8° and 66.8°, correspond to (013), (111), (400) and (440) planes of gamma alumina phases and match closely with the reported values (JCPDS 46-1131). d-lines observed at 2θ values 28.6°, 33.3°, and 56.4° correspond to those for CeO₂ (JCPDS 34-0394). The d-lines at 2θ = 51.3° and 76.1° are due to (200) and (220) planes for Ni metal (JCPDS 04-0850). The major d-line due to Ni metal at 2θ = 44.4° (111) is masked by the (400) line due to alumina. XRD pattern for 8%Cu/5%CeO₂-Al₂O₃ catalyst exhibits d-lines corresponding gamma alumina and ceria phases in addition to those for Cu metal at 2θ = 43.5° and 50.6° 2θ values due to Cu metal (43.3°, 50.4° and 74.2° (JCPDS 85-1326). and Ni (44.4°, 51.3° and 76.1° (JCPDS 04-0850) are close to each other since both have fcc structure. Hence, in the diffractogram for the bimetallic catalyst 6% Ni-2%Cu/5% CeO₂-Al₂O₃, besides the d-lines due to gamma alumina and ceria, the two prominent lines due to Ni and Cu (44.4°, 44.3°) have been masked by intense and broad d-lines due to gamma alumina. Other two minor lines observed at 51.3° and 76.4° possibly represent both Cu and Ni metals. In the case of other two bimetallic catalysts, 4% Ni-4% Cu and 2.5%Ni-5.5%Cu, d lines due to alumina and ceria phases only are seen, since the d-lines due to Cu and Ni have been masked by the lines due to gamma alumina. It is likely that both Ni and Cu are highly dispersed, since ceria is known to improve dispersion of the metals. Though Ni-Cu alloy formation during reduction is possible, due to masking by the d-lines due to alumina phase, it is not reflected in the diffractograms.

Textural properties

Nitrogen adsorption-desorption isotherms at - 196 °C and the corresponding pore size distribution curves for the catalysts according to BJH method are presented in Fig. S1. Textural properties of the catalysts are compiled in Table 1. All catalysts display Type IV adsorption desorption isotherms and Type H1 hysteresis loops, indicating that the pores are mesoporous in character and cylindrical in shape. Introduction of Ni and Cu has not brought in any significant change in textural properties since the metal loadings are less (at 8% max) and thermal treatments are carried out at the same conditions.

Table 1 Textural properties of Ni-Cu bi-metallic catalysts

Catalysts	Surface area (m ² /g)	Pore volume (cm ³ /g)	Pore diameter (nm)
5% CeO ₂ -Al ₂ O ₃	136	0.38	11.3
8%Ni/5%CeO ₂ -Al ₂ O ₃	129	0.36	8.6
6%Ni -2%Cu/5%CeO ₂ -Al ₂ O ₃	130	0.32	10.5
4%Ni -4%Cu/5%CeO ₂ -Al ₂ O ₃	129	0.34	10.9
2.5%Ni -5.5%Cu/5%CeO ₂ -Al ₂ O ₃	129	0.33	9.9
8%Cu/5%CeO ₂ -Al ₂ O ₃	114	0.34	9.1

Transmission electron microscopy (TEM)

Transmission electron micrographs for the reduced catalysts presented in Fig. S2 show fairly good dispersion of nickel crystallites on the supports. All catalysts exhibit needle shaped morphology as reported in literature for alumina supported nickel-copper catalysts.

Temperature programmed reduction (H_2 -TPR)

H_2 TPR profiles for the three Ni-Cu bimetallic catalysts are presented in Fig. S3 along with those for monometallic Ni and Cu catalysts for comparison. TPR maxima observed for all the catalysts are compiled in Table 2. Three distinct regions/zones of reduction, namely, (i) reduction of free and weakly bound Ni/Cu oxides (Zone I) (ii) reduction of well- dispersed Ni and Cu oxides (Zone II) and (iii) reduction of surface and bulk Ni–Cu aluminates (Zone III) which are formed due to strong interaction with the support are observed. In the case of mono metallic Ni, based on the hydrogen consumption pattern, well-dispersed NiO (in Zone II) appear as the major reducible phase, while free/weakly bound NiO and surface and bulk nickel aluminate phases (in Zone I and Zone III) are revealed as minor phases.

In contrast, in the case of mono metallic copper catalyst, free and weakly bound CuO phases are predominant, indicating that metal support interaction (MSI) is weaker in Cu based catalysts in comparison with MSI in Ni based catalysts. Maxima at 107 °C and 208 °C correspond to reduction of weakly bound Cu^{2+} [17], while maxima at 441 °C and 558 °C due to reduction of dispersed Cu^{2+} . Very small amount of Cu in aluminate phase is observed, as revealed by a minor reduction peak at 672 °C. Introduction of 2% Cu in 2%Cu-6% Ni catalyst increases the reducibility of Ni^{2+} [17–19] as indicated by partial shift of dispersed Ni^{2+} reduction peak from 469 to 464 °C and the remaining dispersed Ni^{2+} getting reduced at 582 °C. A small part of the Ni^{2+} gets reduced at higher temperature due to strong interaction with the support. Simultaneously, low temperature reduction peaks due to weakly bound Cu^{2+} move over to higher temperature region indicating simultaneous reduction of Ni^{2+} and Cu^{2+} in dispersed state [17]. Increasing Cu^{2+} content to 4% in 4%Ni-4%Cu catalyst increases further the reducibility of Ni^{2+} , thus increasing interaction

Table 2 Temperature Programmed Reduction characteristics of Ni-Cu bimetallic catalysts

Catalysts	TPR maxima (°C) Hydrogen consumption (%)		
	Zone-I (100 °C-400°C)	Zone-II (400 °C- 600 °C)	Zone-III (600 °C-800°C)
8%Ni/5%CeO ₂ -Al ₂ O ₃	187,346	489	640, 780
6%Ni-2%Cu/5%CeO ₂ -Al ₂ O ₃	134, 249, 329,386	464, 582	658, 771, 855
4%Ni -4%Cu/5%CeO ₂ -Al ₂ O ₃	112, 228, 353	474, 541	651, 722
2.5%Ni-5.5%Cu/5%CeO ₂ -Al ₂ O ₃	229, 365	494, 552	663, 773
8%Cu/5%CeO ₂ -Al ₂ O ₃	107, 208	441, 558	672

between Ni and Cu and simultaneous reduction of both, resulting in the formation of Ni–Cu alloy phase. This aspect is brought out by two observations, first, maximum reducibility of Ni and Cu at 474 °C and second, shifting of dispersed Ni²⁺ reduction maximum from 582 to 541 °C. Formation of Ni–Cu alloys by simultaneous reduction of Ni and Cu ions could influence facile dehydrogenation and hydrogenation functionalities of the catalyst [14]. Further increase in Cu content in 2.5% Ni–5.5% Cu catalyst results in consolidation of simultaneous reduction and alloy formation of Ni–Cu as indicated by the maxima at 494 °C and 552 °C. With Cu content being high, the intensity of the reduction maxima due to free and weakly bound Cu²⁺ increases indicating high loading of Cu, may lead to its segregation [20]. Simultaneously, high temperature reduction peak due to Cu–Ni aluminate species increases in intensity. TPR data thus show that the gradual incorporation of Cu²⁺ into NiO–Ceria–alumina lattice stabilizes Cu in the lattice, and brings about the interaction between Ni and Cu, leading to the formation of alloys during simultaneous reduction.

X-ray photoelectron spectroscopy (XPS)

XPS profiles for a typical bimetallic catalyst 5.5% Cu–2.5% Ni/CeO₂–Al₂O₃ in reduced state are given in Fig. S4. XPS profiles for core electron states for Al_{2p}, Ce_{3d}, Cu_{2p} and Ni_{2p} are also included. Ni_{2p_{3/2}} peak at 853.1 eV is due to Ni metal in bimetallic catalyst, which is nearly the same as 853.0 eV observed for mono metallic Ni/5% CeO₂–Al₂O₃ Table S4. According to Naghash et al. [14, 20], in Ni–Cu bimetallic catalysts supported on alumina, alloy formation is possible depending on the Cu loading and the reduction temperature and charge transfer from Cu to Ni could lead to lower BE value for Ni. However, it was reported by [20] that such shifts in BE of Ni were seen at lower loading of Cu and at higher Cu loading no change in BE of Ni with respect to Ni metal is observed. In the present case, since Cu loading in 4% Ni–4% Cu catalyst is high, no change in BE value for Ni_{2p} is observed compared to the mono metallic Ni, though alloy formation is indicated in TPR data. Alloy formation in Ni–Cu bimetallic catalysts have been reported in literature. [14, 20, 21]. XPS lines due to Cu_{2p_{3/2}} and Cu_{2p_{1/2}} levels are observed at 929.8 eV and 949.8 eV, respectively, with $\Delta = 20$ eV and intensity ratio ~0.5 indicating the presence of Cu in metallic state. Compared to the reported value of 933 eV for Cu metal, shift in BE to 929.8 eV could be due to the support effect. Weak satellite peak observed at 939.9 eV indicates the presence of small amount of Cu₂O. XPS lines observed at 900.7 eV is due to Ce⁴⁺ 3d_{3/2} level and the one at 892.6 eV is due to Ce⁴⁺ 3d 5/2 level.

Acidity and basicity of the catalysts

TPD profiles for ammonia and CO₂ for monometallic Ni and Cu along with the three Ni–Cu bimetallic catalysts are presented in Fig. S5 and Fig. S6. Peak maxima for the desorption of NH₃ and CO₂, classified as weak, medium and strong acid/basic sites are compiled in Tables 3 and 4. Population of acid/base sites of

Table 3 Distribution of acid sites on bimetallic Ni-Cu catalysts

Catalysts	Distribution of acid sites			
	Weak °C/mmol/g	Medium °C/mmol/g	Strong °C/mmol/g	Total mmol/g
8%Ni/5%CeO ₂ -Al ₂ O ₃	267/0.53	370/0.93	461/0.21	1.67
6%Ni-2%Cu/5%CeO ₂ -Al ₂ O ₃	183/0.04	341/0.701	488/0.04	0.781
4%Ni-4%Cu/5%CeO ₂ -Al ₂ O ₃	189/0.035	343/0.793	513/0.100	0.928
2.5%Ni-5.5%Cu/5%CeO ₂ -Al ₂ O ₃	187/0.068	361/0.836	528/0.079	0.983
8%Cu/5%CeO ₂ -Al ₂ O ₃	175/0.025	341/0.629	491/0.075	0.729

Table 4 Distribution of basic sites on bimetallic Ni-Cu catalysts

Catalysts	Distribution of basic sites			
	Weak °C/mmol/g	Medium °C/mmol/g	Strong °C/mmol/g	Total mmol/g
8%Ni/5%CeO ₂ -Al ₂ O ₃	199/0.019	355/0.132	486/0.014	0.165
6%Ni-2%Cu/5%CeO ₂ -Al ₂ O ₃	115/0.03	362/0.168	577/0.038	0.236
4%Ni-4%Cu/5%CeO ₂ -Al ₂ O ₃	114/0.04	337/0.179	519/0.04	0.259
2.5%Ni-5.5%Cu/5%CeO ₂ -Al ₂ O ₃	212/0.025	357/0.161	539/0.023	0.209
8%Cu/5%CeO ₂ -Al ₂ O ₃	194/0.016	333/0.100	484/0.052	0.168

different strengths and total acidity/basicity in terms of mmol/g of ammonia/CO₂, have been included in the tables.

Total acidity of bimetallic Ni-Cu and mono metallic Cu catalysts is less (0.729–0.983 mmol of NH₃) than that for mono metallic Ni (1.67 mmol of NH₃). Mono metallic Cu and bimetallic Ni-Cu catalysts display relatively weaker acid sites (desorption temperatures 175–189 °C) compared to mono metallic Ni (267 °C) and less in site population (0.025–0.068 vs 0.53 mmol of NH₃/g). Desorption temperatures for medium strength acid sites are in narrow temperature range, (341–370 °C) revealing that these sites are of nearly same strength across the series and so also the population of such sites. However, the three bimetallic Ni-Cu catalysts and mono metallic Cu display relatively stronger acid sites with desorption temperatures higher (488–528 °C) than mono metallic Ni catalyst at 461 °C, but the population of such stronger sites is less, 0.04–0.1 vs 0.21 mmol of NH₃/g for mono metallic Ni. Introduction of Cu in Ni/CeO₂-Al₂O₃ thus results in moderation of overall acidity and generation of weaker acid sites.

Total basicity of Ni-Cu bimetallic catalysts is slightly higher than the two mono metallic catalysts. While there are no significant changes in terms of strength or population of weak and medium strength basic sites, stronger basic sites (with desorption temperatures (519–577 °C) are observed with bimetallic catalysts compared to mono metallic catalysts (with desorption temperatures 484

and 486 °C). Majority of basic sites in Ni–Cu bimetallic catalysts are of medium strength, along with small amounts of stronger basic sites.

Conversion of ethanol into higher carbon number alcohols

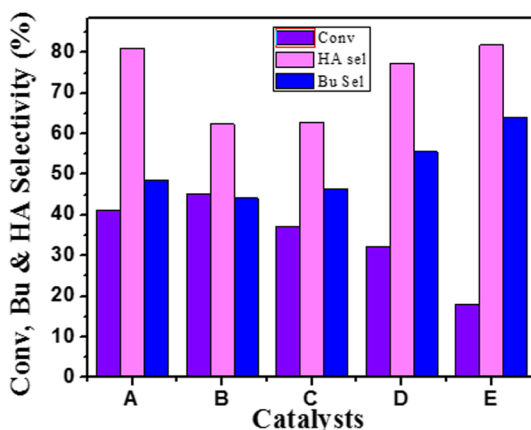
Distribution of products

Graphical representation of the data on the conversion of ethanol and selectivity to butanol and higher carbon number alcohols at 200 °C on Ni–Cu series of bimetallic catalysts supported on ceria modified alumina is presented in Fig. 2 and the respective values are compiled in Table S5 for ready reference. Major products obtained include butanol, hexanol and octanol with ethylene as the major by product along with small amounts of C_1 – C_5 hydrocarbons and oxides of carbon. Besides C_2 – C_8 aldehydes, ketones and esters are observed in trace amounts. Small amounts of acetaldehyde and butyraldehyde in the product stream for Ni–Cu bimetallic catalysts indicate that the process follows typical Guerbet chemistry pathway. Thus, overall product pattern and hence reaction pathway in the case of Ni–Cu catalysts is similar to the ones observed in mono metallic Ni, and Cu catalysts.

Trends in ethanol conversion and selectivity

While mono metallic Ni displays higher ethanol conversion of 41.1%, monometallic Cu shows very low conversion of 18% under identical reaction conditions. Lower ethanol conversion of alumina supported Cu vs Ni was reported by [22], who have investigated ethanol conversion on alumina supported Ni (16% and 19% loading) Co (16% loading) and Cu (1.5% and 4.5% loading) in continuous flow mode at 240 °C and 70 bar pressure. While the conversion was 27% and 25% on Co and Ni catalysts, respectively, it was only 12–14% on Cu catalysts. Butanol selectivity observed

Fig. 2 Activity data for Ni–Cu bimetallic catalysts
 A) 8%Ni/5%CeO₂-Al₂O₃, B) 6%Ni-2%Cu/5%CeO₂-Al₂O₃, C) 4%Ni-4%Cu/5%CeO₂-Al₂O₃, D) 2.5%Ni-5.5%Cu/5%CeO₂-Al₂O₃, E) 8%Cu /5%CeO₂-Al₂O₃



was 60–65% on Co and Ni catalysts and 55–65% on Cu under their reaction conditions. Literature data on copper-based catalysts for condensation of ethanol, compiled in Table S3, show that the activity/conversion depends on the type of the supports used. It is observed Cu based catalysts with alumina/modified alumina supports display lower ethanol conversion. However, Cu when supported on HTC type Mg–Al–O oxides (PMO—porous metal oxides) [14] are fairly active, with 37.8% conversion, albeit at higher temperatures, at 310 °C. In the case of ceria promoted Cu catalyst on different supports, [23] observed that Cu supported on ceria modified activated carbon (AC) displayed higher conversion when compared alumina or silica supported Cu catalysts. Presence of Cu in Cu^+ state on these supports is considered to be responsible for low activity of Cu.

In the present case, XPS data on 8% Cu/CeO₂–Al₂O₃ does indicate the presence of Cu^+ (Cu_2O phase) in small amount. [22] Also observed presence of Cu^{2+} in aluminate phase. In the case of Cu/AC catalysts, complete reduction of Cu to metallic state is achieved so that all Cu in metallic phase is available for dehydrogenation/hydrogenation steps. With reactive supports like alumina/modified alumina, due to fairly strong metal-support interactions, part of Cu is not in reduced state and hence, the first step in the Guerbet process, namely, dehydrogenation of ethanol to acetaldehyde, is relatively slow in comparison with Ni/CeO₂–Al₂O₃. This aspect explains lower ethanol conversion observed with monometallic Cu observed in the present work, compared to mono metallic Ni and Co.

Data presented in Fig. 2 and Table S5, show that replacement of 2% Ni with 2% Cu, has resulted in slight increase in ethanol conversion from 41.1 to 45.1% with a concomitant decrease in butanol and higher alcohol selectivity. On further increase in Cu to 4%, ethanol conversion decreases significantly, to 37%. In both cases, butanol and higher alcohol selectivity are nearly the same. With increase in Cu content to 5.5% ethanol conversion decreases further to 32% while selectivity to butanol and higher alcohols increases significantly, to 55.6% and 77.3%.

Increase in conversion is seen only when Cu loading is 2% and at higher Cu loading activity decreases. Formation of Ni–Cu alloy (as indicated by TPR and XPS studies) could be responsible for the increase in ethanol conversion and formation of butanol and higher alcohols [14]. In the present case, it is likely that the effect of alloying on activity is seen only with lower loading of Cu. Besides, as indicated in acidity and basicity data for Ni–Cu catalysts, (Tables 3 and 4) generation of weaker acidic and basic sites and stronger acidic and basic sites across the Ni–Cu series is another factor responsible for higher butanol and higher alcohol selectivity. Presence of weaker acid sites and decrease in total acidity in Ni–Cu bimetallic catalysts is responsible for nearly constant selectivity observed for ethyl acetate. However, substantial decrease in selectivity for ethylene is observed as Cu content increases which could be due to decrease in overall acidity across the series (Table S6). With maximum butanol selectivity of 55.6%, the catalyst formulation 2.5%Ni-5.5%Cu/5%CeO₂–Al₂O₃ shows butanol yield of 17.9% at low reaction temperature of 200 °C. Other catalysts like Ni10Cu10-PMO (21.1%) and Cu-HASCeO₂ (30%) display higher yields at severe process conditions like 310 °C/80 bar pressure and supercritical CO₂ process conditions. Further optimization of Cu–Ni composition could result in higher butanol yield. Recently, [24] could achieve 44% ethanol

conversion, 75% selectivity at 300–350 °C and WHSV-0.1–0.2 h⁻¹ with Cu/MgO-Al₂O₃ catalyst.

Conclusions

A series of bimetallic Ni–Cu catalysts supported on ceria modified alumina have been prepared and characterized by XRD, TPR, XPS and acidity-basicity measurements. Formation of Ni–Cu alloys at specific compositions, as indicated by TPR and XPS results, leads to the promotion of dehydrogenation-hydrogenation function of the process. Generation of weaker acid sites and stronger basic sites, when compared to mono metallic Ni and Cu catalysts, results in improvements in the selectivity for butanol and higher carbon number alcohols. Bimetallic catalyst with composition 5.5% Cu-2.5% Ni displays maximum butanol selectivity of 55.6% and total higher alcohol selectivity of 77.3% among the series of catalysts and at lower reaction temperature of 200 °C. Other Ni–Cu bimetallic catalysts reported in literature are active at temperatures > 300 °C. Further optimization of Cu and Ni composition and support acidity/basicity, could result in catalysts with better performance. Design of bimetallic catalysts with optimum composition is an useful strategy for improving overall process efficiency.

Supplementary Information The online version contains supplementary material available at <https://doi.org/10.1007/s11144-023-02347-6>.

Acknowledgements The authors are grateful to DST, GOI, New Delhi, for providing the research facilities at NCCR, IIT Madras, Chennai and adequate instrumentation facilities for characterization of catalysts in the Department of Chemistry, Anna University, Chennai.

Data availability There is no additional data available. All other data are available from the authors upon reasonable request.

Declarations

Conflict of interest No conflict of interests among the authors.

References

1. Guerbet M (1901) The action of ethyl alcohol on baryta ethylate, and synthesis of the normal butylic alcohol. *C R Hebd Seances Acad Sci* 133:300–302
2. Harvey BG, Meylemans HA (2011) The role of butanol in the development of sustainable fuel technologies. *J Chem Technol Biotechnol* 86:2–9
3. Xue C, Zhao XQ, Liu CG, Chen LJ, Bai FW (2013) Prospective and development of butanol as an advanced biofuel. *Biotechnol Adv* 31:1575–1584
4. Thompson R, Behnam M, Swana J, Yang Y (2011) An analysis of net energy production and feedstock availability for biobutanol. *Bioresour Technol* 102:2112–2117
5. Singh SB, Dhar A, Agarwal AK (2015) Technical feasibility study of butanol-gasoline blends for powering medium-duty transportation spark ignition engine. *Renew Energy* 76:706–716
6. Derre P (2007) Biobutanol: an attractive biofuel. *Biotechnol J* 2:1525–1534
7. Ndaba BI, Chiyanzu I, Marx S (2015) *Biotechnol Rep* 8:1
8. Nexant Inc. (2015) Petrochemical market dynamics Oxo alcohols. Nexant Inc, San Francisco.

9. Eagan NM, Kumbhalkar MD, Buchanan JS, Dumesic JA, Huber GW (2019) Chemistries and processes for the conversion of ethanol into middle-distillate fuels. *Nat Rev Chem* 3:223–249
10. Han GB, Jang JM, Hwei-Ahn M, Jung BH (2019) Bio-Jet Fuel Inetch Open
11. Kozłowski JD, Davis RJ (2013) Heterogeneous catalysts for the guerbet coupling of alcohols. *ACS Catal* 3:1588–1600
12. Aitchison H, Wingad RL, Wass DF (2016) Homogeneous ethanol to butanol catalysis-guerbet renewed. *ACS Catal* 6:7125–7132
13. Wu X, Fang G, Tong Y, Jiang D, Liang Z, Leng W, Liu L, Tu P, Wang H, Ni J, Li X (2018) Catalytic upgrading of ethanol to n-butanol: Progress in catalyst development. *Chemsuschem* 11:71–85
14. Sun Z, Couto Vasconcelos A, Bottari G, Stuart MCA, Bonura G, Cannilla C, Frusteri F, Barta K (2017) Efficient catalytic conversion of ethanol to 1-butanol via the guerbet reaction over copper and nickel doped porous. *ACS Sustain Chem Eng* 5:1738–1746
15. Vinayagamoorthi R, Krishnamurthy KR, Viswanathan B, Shanthi K (2021) Ethanol condensation to butanol and higher alcohols over nickel and cobalt decorated CeO₂-Al₂O₃ mixed oxide catalysts. *Indian J Chem* 60:386–396
16. Vinayagamoorthi R, Shanthi K, Thirunavukkarasu K, Krishnamurthy KR, Viswanathan B (2021) Conversion of ethanol to higher alcohols on Ni/M_xO_y-Al₂O₃ (M=La, Ce, Zr, Mg & Ti) catalysts-Influence of support characteristics. *Indian J Chem Technol* 28:9–22
17. Hernandez WY, De Vlieger K, Van Der Voort P, Verberckmoes An (2016) Ni-Cu hydrotalcite-derived mixed oxides as highly selective and stable catalysts for the synthesis of b-branched bioalcohols by the guerbet reaction. *Chemsuschem* 9:3196–3205
18. Loredana DR, Tiziano Montini T, Barbara Lorenzuti B, Paolo Fornasiero P (2008) Ni_xCu_y/Al₂O₃ based catalysts for hydrogen production. *Energy Environ Sci* 1:501–509
19. Rodriguez A, Jirsak T, Pérez M (2001) Studies on the behavior of mixed metal oxides: adsorption of CO and NO on MgO (100), and Ni_xMg_{1-x}O(100) and Cr_xMg_{1-x}O (100). *J Chem Phys* 9:1
20. Naghash AR, Etsell TH, Xu S (2006) XRD and XPS study of Cu- Ni interactions on reduced copper-nickel-aluminum oxide solid solution catalysts. *Chem Mater* 18:2480–2488
21. Khromova SA, Smirnov AA, Bulavchenko OA, Saraev AA, Kaichev VV, Reshetnikov SI, Yakovlev VA (2014) Anisole hydrodeoxygenation over Ni–Cu bimetallic catalysts: the effect of Ni/Cu ratio on selectivity. *Appl Catal A* 470:261–270
22. Riittonen T, Ernen K, M-ki-Arvela P, Shchukarev A, Rautio AR, Kordas K, Kumar N, Salmi T, Mikkola JP (2015) Continuous liquid-phase valorization of bio-ethanol towards bio-butanol over metal modified alumina. *Renewable Energy* 74:369–378
23. Jordison TL, Lira CT, Miller DJ (2015) Condensed-phase ethanol conversion to higher alcohols. *Ind Eng Chem Res* 54:10991–11000
24. Ruddy, D, Dagle, R, Li Z (2019) Liquid Fuels via Upgrading of Indirect Liquefaction Intermediates

Publisher's Note Springer Nature remains neutral with regard to jurisdictional claims in published maps and institutional affiliations.

Springer Nature or its licensor (e.g. a society or other partner) holds exclusive rights to this article under a publishing agreement with the author(s) or other rightsholder(s); author self-archiving of the accepted manuscript version of this article is solely governed by the terms of such publishing agreement and applicable law.